



HAL
open science

Autologous endothelial progenitor cell therapy improves right ventricular function in a model of chronic thromboembolic pulmonary hypertension.

Fanny Loisel, Bastien Provost, Julien Guihaire, David Boulate, Nassim Arouche, Myriam Amsallem, Jennifer Arthur Ataam, Benoît Decante, Peter Dorfmueller, Elie Fadel, et al.

► To cite this version:

Fanny Loisel, Bastien Provost, Julien Guihaire, David Boulate, Nassim Arouche, et al.. Autologous endothelial progenitor cell therapy improves right ventricular function in a model of chronic thromboembolic pulmonary hypertension.. *Journal of Thoracic and Cardiovascular Surgery*, 2018, 157 (2), pp.655-666. 10.1016/j.jtcvs.2018.08.083 . inserm-02401995

HAL Id: inserm-02401995

<https://inserm.hal.science/inserm-02401995>

Submitted on 21 Oct 2021

HAL is a multi-disciplinary open access archive for the deposit and dissemination of scientific research documents, whether they are published or not. The documents may come from teaching and research institutions in France or abroad, or from public or private research centers.

L'archive ouverte pluridisciplinaire **HAL**, est destinée au dépôt et à la diffusion de documents scientifiques de niveau recherche, publiés ou non, émanant des établissements d'enseignement et de recherche français ou étrangers, des laboratoires publics ou privés.



Distributed under a Creative Commons Attribution - NonCommercial 4.0 International License

1 **Abstract Word Count:** 216

2 **Text Word Count:** 3478

3 **Title: Autologous Endothelial Progenitor Cell Therapy Improves Right Ventricular**
4 **Function in a Model of Chronic Thromboembolic Pulmonary Hypertension**

5 **Authors:** *Fanny Loisel, MSc^{1,2}; *Bastien Provost, MD, MSc¹; Julien Guihaire, MD, PhD^{1,3};
6 David Boulate MD^{1,4}; Nassim Arouche, Eng²; Myriam Amsallem MD¹, Jennifer Arthur-
7 Ataam PhD¹, Benoît Decante, MSc¹; Peter Dorfmueller MD PhD^{1,6}; Elie Fadel, MD, PhD^{1,4,5};
8 Georges Uzan, PhD²; and Olaf Mercier, MD, PhD^{1,4,5}

9 1- Research and Innovation Unit, Inserm UMR-S 999, Marie Lannelongue Hospital,
10 Univ. Paris Sud, Paris-Saclay University, Le Plessis Robinson, France

11 2- Inserm 1197 Research Unit, 94807 Villejuif Cedex, France Univ. Paris Sud, Paris-
12 Saclay University, France

13 3- Department of Cardiac Surgery, Marie Lannelongue Hospital, Univ. Paris Sud, Paris-
14 Saclay University, Le Plessis Robinson, France

15 4- Department of Thoracic and Vascular Surgery and Heart-Lung Transplantation, Marie
16 Lannelongue Hospital, Univ. Paris Sud, Paris-Saclay University, DHU TORINO, Le
17 Plessis Robinson, France

18 5- Paris-Sud University and Paris-Saclay University, School of Medicine, Kremlin-
19 Bicêtre, France

20 6- Department of Pathology, Marie Lannelongue Hospital, Le Plessis Robinson, France

21 *Contributed equally to this work

22 Corresponding Author: Olaf Mercier, MD, PhD, Department of Thoracic and Vascular
23 Surgery and Heart-Lung Transplantation, Research and Innovation Unit, Marie Lannelongue

24 Hospital, 133 Avenue de la Resistance, 92350, Le Plessis Robinson, France. Email:
25 o.mercier@ccml.fr

26 **Conflicting Interest:** The authors declare that there is no conflict of interest.

27

28 **Funding, acknowledgements:** This work was supported by a public grant overseen by the
29 French National Research Agency (ANR) as part of the second ‘Investissement d’Avenir’
30 program (reference: ANR-15-RHUS-0002).

31

32 **Central Message**

33 Coronary infusion of autologous endothelial progenitor cells improved right ventricle
34 adaptation to pulmonary hypertension in an animal model of chronic thromboembolic
35 pulmonary hypertension.

36

37 **Perspective Statement**

38 Pulmonary hypertension is a life-threatening disease that leads to right ventricle failure. To
39 date, pharmacological advances have targeted the pulmonary circulation. We report that right
40 ventricle-targeted cell therapy may hold promise in supporting right ventricular function in a
41 model of chronic thromboembolic pulmonary hypertension.

42

43 **Abbreviations**

44 PH: Pulmonary Hypertension

45 CTEPH: Chronic Thromboembolic Pulmonary Hypertension

46 RV: Right Ventricular

47 LV: Left Ventricle

48 VA: Ventriculo-Arterial

49 EPCs: Endothelial Progenitor Cells

50 MNCs: MonoNuclear Cells

51 FACS: Fluorescence-Activated Cell Sorting

52 PAP: Pulmonary Arterial Pressure

53 TPR: Total Pulmonary Resistance

54 Ees: End-systolic elastance

55 Ea: Arterial elastance

56 RUL: Right Upper Lobe

57 MHC: Myosin Heavy Chain

58 BMCs: Bone Marrow Cells

59

60

61

62

63 **Abstract:**

64 *Background:* Right ventricular (RV) failure is the main prognostic factor in pulmonary
65 hypertension (PH), and ventricular capillary density (CD) has been reported to be a marker of
66 RV maladaptive remodeling and failure. Our aim was to determine whether right
67 intracoronary Endothelial Progenitor Cells (EPCs) infusion can improve RV function and CD
68 in a piglet model of Chronic Thromboembolic Pulmonary Hypertension (CTEPH).

69 *Methods:* We compared three groups: Sham (n=5), CTEPH (n=6), and CTEPH+EPC (n=5).
70 Following EPC isolation from CTEPH+EPC piglet peripheral blood samples at three weeks,
71 CTEPH and Sham groups underwent right intracoronary infusion of saline, while the
72 CTEPH+EPC group received EPCs at six weeks (T6). RV function, pulmonary
73 hemodynamics, and myocardial morphometry were investigated in the animals at ten weeks
74 (T10).

75 *Results:* Following EPC administration, the right ventricular fractional area change increased
76 from 32.75% (29.5-36.5) to 39% (37.25-46.50), $p=0.030$. The CTEPH+EPC piglets had
77 reduced cardiomyocyte surface areas (from 298.3 (277.4-335.3) to 234.6 (211.1-264.7),
78 $p=0.017$), and increased CD31 expression (from 3.12 (1.27-5.09) to 7.14 (5.56-8.41)
79 $p=0.017$). EPCs were found in the RV free wall at 4 h and at 24 h after injection but not four
80 weeks later.

81 *Conclusion:* Intracoronary infusion of EPC improved RV function and CD in a piglet model
82 of CTEPH. This novel cell-based therapy may represent a promising RV-targeted treatment in
83 PH patients.

84

85 **Introduction**

86 Right ventricular (RV) function is the main prognostic factor in pulmonary
87 hypertension (PH) (1). Increased pulmonary vascular resistance induces RV remodeling from
88 an adaptive to a maladaptive phenotype as the disease progresses. Unlike adaptive
89 remodeling, maladaptive RV remodeling is characterized by dilatation, reduced cardiac
90 output, ventriculo-arterial uncoupling, and a high mortality rate. At the cellular level,
91 maladaptive remodeling is associated with reduced angiogenesis, increased fibrosis, metabolic
92 changes, and a dysregulation of the autonomic nervous system (2) (3). The transition from
93 adaptive to maladaptive RV remodeling is a continuum that ultimately leads to end-stage
94 heart failure.

95 A decrease in ventricular capillary density occurs in various animal models of PH (4)
96 (5) and in humans at the stage of maladaptive remodeling or heart failure (6). Indeed, RV
97 ischemia has been described by Gómez et al. in the setting of chronic PH (7). To date, no cell
98 based therapy is available for the overloaded RV. Therefore, Endothelial Progenitor Cells
99 (EPCs) may be good candidates for RV-targeted therapy as they can differentiate into
100 specialized endothelial cells (8) and since they release paracrine factors involved in
101 angiogenesis (9). EPCs have been reported to promote vascular repair and angiogenesis (10)
102 (11) (12), although they have not yet been investigated in PH.

103 Chronic Thromboembolic Pulmonary Hypertension (CTEPH) is characterized by
104 chronic pulmonary vessel obstruction combined with severe distal vasculopathy (13). Our
105 group developed a novel piglet model of CTEPH that has been validated both for RV
106 dysfunction and pulmonary vascular disease (14) (15). We reported that ventricular-arterial
107 uncoupling can be durably reversed when the RV afterload is normalized in this large-animal
108 model (16). Moreover, the RV capillary density is impaired in long-term CTEPH animal
109 models (17). Consequently, our aim was to investigate the effect of right intracoronary

110 administration of EPCs on RV function and capillary density. Our hypothesis was that EPC
111 would improve RV function by enhancing capillary density.

112

113 **Methods**

114 *Chronic thromboembolic pulmonary hypertension model*

115 Five-week-old large white piglets, weighing 20-22 kg, were included in the
116 preliminary (n=2) and the main study (n=16). The animals were randomly assigned to Sham
117 or CTEPH groups. To establish the CTEPH model, the piglets were first subjected to surgery
118 under general anesthesia (propofol, isoflurane, and pancuronium) and mechanical ventilation,
119 and they underwent a ligation of the left pulmonary artery through a left thoracotomy.
120 Embolization of the right pulmonary artery was then performed weekly over a five-week
121 period, via percutaneous access to the brachiocephalic vein, using cyanoacrylate glue
122 (Histoacryl®, B. Braun, Melsungen, Germany), to target the right lower lobe (14). Thus,
123 ligation of the left pulmonary artery, combined with selective occlusion of the distal arteries
124 of the right lower lobe, gradually increased the pulmonary vascular resistance, thereby leading
125 to RV dysfunction at five weeks. The animals in the Sham group underwent a thoracotomy
126 and weekly right pulmonary artery saline injections over a five-week period to mimic the
127 embolization of the animals in the CTEPH group.

128 A preliminary pilot study was undertaken using one Sham piglet in which GFP-
129 labelled EPCs were administrated at six weeks (T6), and the animal was sacrificed 4 h later.
130 One CTEPH piglet received GFP-labelled EPCs at T6 and it was sacrificed 24 h later.

131 Sixteen piglets were included in the main study: 5 Sham, 6 CTEPH, and 5
132 CTEPH+EPC (Fig. 1a). At T6, the animals in the Sham and the CTEPH groups received a
133 right intracoronary injection of saline, whereas the animals in the CTEPH+EPC group each

134 received 16 ± 3.21 million GFP-labelled EPCs (an average of 6.5×10^4 EPC/kg) (Fig. 1b).
135 Animals entering the CTEPH procedure were randomly assigned to either the CTEPH or the
136 CTEPH+EPC group at the time that the model was established, just before to the left
137 pulmonary artery ligation.

138 *EPC administration*

139 Cell therapy administration was performed at T6 for the CTEPH+EPC group. This
140 time point was chosen because it has been proven in the study of Mercier et al. that chronic
141 PH is developed in pigs 5 weeks after left PA ligation and weekly embolization (14). EPC
142 administration was performed under general anesthesia, using a 4-French catheter inserted
143 through the femoral artery and an AR I mod catheter (Cordis) placed in the proximal right
144 coronary artery, under fluoroscopic guidance. Proper positioning of the catheter was assessed
145 by injection of contrast agent. Autologous EPCs were resuspended in 20 mL of saline solution
146 in a syringe, and injected continuously through the catheter into the right coronary artery at a
147 rate of 6.6 mL/min. Each piglet in the CTEPH+EPC group was injected with the maximum
148 number of cells available after culturing for no more than 4 passages.

149 *Hemodynamic assessment*

150 The heart rate, the mean pulmonary artery pressure (mPAP), cardiac output, and blood
151 saturation were measured at baseline (T0), at 6 weeks (T6), and at 10 weeks (T10).

152 A pressure-volume loop analysis of the RV was performed at T6 and T10 with a
153 conductance VentriCath 507 (Millar Instruments, Houston, TX, USA).

154 *Echocardiographic assessment*

155 Transthoracic echocardiography (Vivid E9; GE Medical Systems Milwaukee, WI,
156 USA) was performed at T0, T6, and T10. Tricuspid Annular Plane Systolic Excursion

157 (TAPSE), right ventricular fractional area change (RVFAC), and the RV free wall strain were
158 assessed (18). Measurements were analyzed by two blinded cardiologists.

159 *Capillary density assessment in the RV*

160 To assess the capillary density (CD), RV samples were incubated with a rabbit anti-
161 human CD31 (CD31 clone 1A10, 1:100, Diagnostics, Blagnac, France) detected by ultraView
162 Universal DAB Detection Kit (Ventana, California USA) staining with Benchmark GX
163 (Roche, Boulogne-Billancourt, France). The CD was determined by the number of capillaries
164 per mm² in five fields of view for each animal at 400x (NIS-Element software, Nikon).

165 *Cardiomyocyte surface assessment in the RV*

166 RV samples were incubated with wheat germ agglutinin (WGA-AF488, Invitrogen,
167 USA, 10 µg/mL) and DAPI (1:10,000, Sigma-Aldrich, Missouri, USA). The cardiomyocyte
168 surface was determined, as previously described (19), using ImageJ software in 15 fields of
169 view for each animal at 630x (NIS-Element software, Nikon).

170 *Statistical analysis*

171 Data from the three groups were compared with the Kruskal-Wallis test, and the groups were
172 compared two by two with the Mann-Whitney test in case of a significant Kruskal-Wallis test.
173 The results are presented as medians (interquartile range (IQR)). Statistical analyses were
174 performed using Prism 6 software (GraphPad® software, San Diego, California, USA).

175 See Supplemental Methods and Supplemental Fig. 1 and Fig. 2 for more details.

176

177 **Results**

178 *Preliminary study*

179 The aim of the preliminary study was to evaluate the feasibility and safety of right
180 intracoronary administration of EPCs in piglets. We observed neither ischemic areas,
181 perivascular inflammatory infiltrates, nor scarring in the tissue (data not shown). A Sham
182 piglet was sacrificed 4 h and a CTEPH piglet was sacrificed 24 h after receiving EPCs
183 through the right coronary artery. Immunohistological analysis revealed the presence of EPCs
184 in the RV myocardium and capillaries as well as in the RUL (Fig. 2). EPCs were also found in
185 the spleen, albeit at a lower level (data not shown).

186 *Assessment at six weeks (T6)*

187 There was no difference in terms of body weight, body surface area, and hemodynamic data
188 (mPAP, TPR, cardiac output, right ventricular fractional area change, TAPSE, RV free wall
189 strain, and Ees/Ea) between the CTEPH and CTEPH+EPC groups at T0 and at T6 (data not
190 shown).

191 *Assessment of EPC function*

192 Analysis of the EPC expression markers revealed no difference between the control
193 EPCs and the CTEPH-EPCs (see Supplemental Fig. 3). In terms of EPC function, there was
194 no difference between the control EPCs and the CTEPH-EPCs in terms of Ac-LDL uptake
195 (Supplemental Fig. 4), wound healing closure (Supplemental Fig. 5), and proliferation
196 (Supplemental Fig. 6a, b, c).

197 *RV function and pulmonary hemodynamics*

198 Intracoronary administration of EPCs in the CTEPH animals was determined to be safe and
199 feasible (e.g., no arrhythmia, myocardial infarction, or sudden death following the procedure).
200 Pulmonary hemodynamic as well as RV function were stable during the experiment, and the
201 cardiac troponin I blood level returned to within the normal range four weeks (T10) after EPC
202 infusion (Supplemental Fig. 7).

203 At T10, the RVFAC was not significantly different between the Sham (43.5% (33.75-45.48))
204 and both the CTEPH (32.7% (29.5-36.5)) and the CTEPH+EPC groups (39% (37.25-46.5))
205 (Sham vs. CTEPH $p=0.125$ and Sham vs. CTEPH+EPC $p=0.889$). However, the RVFAC was
206 significantly higher in the CTEPH+EPC group compared to the CTEPH group ($p=0.030$) (Fig.
207 3a). TAPSE and RV free wall strain were higher in the Sham group compared to both the
208 CTEPH group and the CTEPH+EPC group (TAPSE: 21 mm (19.5-21), 15.5 mm (13.75-
209 17.25), and 16 mm (15.5-17), respectively, Sham vs. CTEPH $p=0.009$ and Sham vs.
210 CTEPH+EPC $p=0.007$; RV free wall strain: 33% (28.6-36), 19.5% (15.5-27.25), and 24%
211 (23.5-29), respectively, Sham vs. CTEPH $p=0.017$ and Sham vs. CTEPH+EPC $p=0.031$).
212 However, the TAPSE and RV free wall strain were not statistically different between the
213 CTEPH group and the CTEPH+EPC group ($p=0.58$ and $p=0.11$ respectively) (Supplemental
214 Fig. 8a, b). In regard to pulmonary hemodynamics, both the mPAP and the TPR indexed to
215 the body surface area remained significantly lower in the Sham group compared to both the
216 CTEPH group and the CTEPH+EPC group (mPAP: 15 mmHg (14.5-17.5), 26 mmHg (23-
217 28), and 24 mmHg (21.5-31), respectively, Sham vs. CTEPH $p=0.008$ and Sham vs.
218 CTEPH+EPC $p=0.016$; TPR: 211.6 dynes.s.cm⁻⁵ (161.1-289.5), 525.8 dynes.s.cm⁻⁵ (458.1-
219 581.4), and 510.9 dynes.s.cm⁻⁵ (451.7-672.1), respectively, Sham vs. CTEPH $p=0.004$ and
220 Sham vs. CTEPH+EPC $p=0.007$). These hemodynamic parameters did not differ significantly
221 between the CTEPH group and CTEPH+EPC group (for mPAP: $p=0.90$ and for TPR: $p=0.77$)
222 (Fig. 3b and 3c). Lastly, the ventriculo-arterial coupling ratio (Ees/Ea) was significantly
223 reduced in the CTEPH group (0.69 (0.56-0.83)) compared to the Sham group (1.03 (0.92-
224 1.05)) ($p=0.008$). The absence of significant difference between the Sham and the
225 CTEPH+EPC group (0.88 (0.67-1.20)) for the Ees/Ea ratio was indicative of a tendency for
226 improved ventriculo-arterial coupling after EPC administration (Fig. 3d). The RVSWI did not
227 differ between the three groups (Sham 685 (596.1-932.6), CTEPH 1202 (967.8-1370), and

228 CTEPH+EPC 868.2 (841.2-1316)) (Fig. 3e). Hemodynamic and echocardiography data have
229 been summarized in a Table 1.

230 *RV and lung morphometry*

231 The pulmonary artery media thickness in the RUL was greater in the CTEPH group (59.9%
232 (53.3-64.6)) and the CTEPH+EPC group (62.4% (54-71.3)) compared to the Sham group
233 (25.3% (22-27.6)), (CTEPH vs. Sham $p < 0.0001$, CTEPH+EPC vs. Sham $p < 0.0001$), while
234 there was no significant difference between the CTEPH animals and the CTEPH+EPC
235 animals ($p = 0.44$) (Fig. 4a, 4b, 4c, 4d). The cardiomyocyte surface area was higher in the
236 CTEPH group ($298.3 \mu\text{m}^2$ (277.4-335.3)) compared to the Sham group ($212.5 \mu\text{m}^2$ (196.8-
237 260.1)) ($p = 0.008$). Interestingly, the cardiomyocyte surface area was lower in the
238 CTEPH+EPC group ($234.6 \mu\text{m}^2$ (211.1-264.7)) compared to CTEPH group ($298.3 \mu\text{m}^2$
239 (277.4-335.3)) ($p = 0.017$). There was no difference between the Sham group and the
240 CTEPH+EPC group ($p = 0.66$) (Fig. 4f, 4h, 4i, 4j). Cardiomyocyte hypertrophy was also
241 evaluated by the α/β MHC ratio. This ratio was significantly lower in the CTEPH group (0.71
242 (0.49-1.06)) compared to the Sham group (2.6 (1.87-5.25)) ($p = 0.004$). However, α/β MHC
243 ratio was not different after EPC administration (CTEPH+EPC 3.90 (0.58-7.21), CTEPH vs.
244 CTEPH+EPC $p = 0.18$) (Fig 4f). No EPCs could be detected in the RV at 10 weeks, whether
245 by histological assessment (data not shown), analysis of GFP expression by Western blot
246 (Supplemental Fig. 9), or RT-qPCR. However, some EPCs were found in the RUL (Fig. 4k)
247 and in the spleen (Fig. 4l).

248 *RV capillary density*

249 CD31 immunohistochemical analysis revealed a higher capillary density (capillary/ mm^2) in
250 the CTEPH group (183.5 (150.1-215.7)) and CTEPH+EPC group (210.6 (190.8-228.4))
251 compared to the Sham group (133.9 (125.2-137.9)) (CTEPH vs. Sham $p < 0.0001$ and

252 CTEPH+EPC vs. Sham $p < 0.0001$). There was a trend toward a higher capillary density in the
253 CTEPH+EPC group compared to CTEPH group ($p = 0.06$). CD31 protein quantification
254 revealed increased CD31 expression (CD31/GAPDH expression) in the CTEPH+EPC group
255 (7.14 (5.56-8.41)) compared to the Sham group (1.256 (0.81-1.88)) ($p = 0.008$) and the CTEPH
256 group (3.12 (1.27-5.08)) ($p = 0.017$) (Fig. 5a-e). The expression of VEGF-A protein was
257 markedly increased (VEGF-A/GAPDH expression) in the CTEPH group (0.22 (0.21-0.27))
258 and the CTEPH+EPC group (0.29 (0.24-0.33)) compared to the Sham group (0.14 (0.18-
259 0.17)) (CTEPH vs. Sham $p = 0.004$, CTEPH+EPC vs. Sham $p = 0.008$) (Fig. 5f).

260

261 **Discussion**

262 Autologous intracoronary injection of EPCs was associated with an improvement in
263 RV systolic function in an animal model of CTEPH. A reduced cardiomyocyte surface area
264 and a tendency for increased capillary density after EPC administration were also observed.
265 EPCs were present in the RV and RUL 4 h and 24 h following their injection in a Sham and a
266 CTEPH piglet, respectively. However, at four weeks they were only discernible in the RUL
267 and spleen. No differences were observed between the CTEPH and the CTEPH+EPC piglets
268 in terms of mPAP and TPR, as well as pulmonary artery remodeling. Although the
269 mechanistic evidence is limited, our results suggest that EPCs may exert their effect mainly
270 on the RV. Indeed, our results are consistent with a primary effect of EPCs on the RV based
271 on improvement of the right ventricular fractional area change and the prevention of
272 hypertrophy in the CTEPH+EPC group. We hypothesize that when EPCs are injected
273 intracoronary they pass through the RV for at least the first 24 h, during which they may
274 secrete paracrine factors leading to a decrease in the cardiomyocyte surface area and a minor
275 increase in capillary density that results in an improvement of the RV hemodynamic function.

276 It should be noted that these are hypotheses, further studies are required to test these
277 assumptions.

278 Intracoronary administration of stem cells has been shown to be safe and feasible (20).
279 Promising results have been obtained in terms of improvement of left ventricular function in
280 patients with heart failure such as myocardial infarction (21) and dilated cardiomyopathy (22),
281 even though in some cases the true effectiveness of the cell therapy is debatable. Using a
282 porcine model of CTEPH, we showed that intracoronary administration of EPCs is safe and
283 feasible (e.g., no arrhythmia, myocardial infarction, or sudden death following the procedure).
284 In keeping with previous studies that used an intracoronary delivery route (23), there was low
285 cell retention at four weeks. The observed absence of EPC was not due to a lack of GFP
286 expression over time as GFP was transmitted to the daughter cells after cell division. Low cell
287 retention is one of the major drawback of intracoronary administration as a result, in this case,
288 it may not be the optimal route of administration.

289 To our knowledge we are the first to administer EPCs directly into the RV of a PH
290 model (24). To date, most of the other EPC therapy studies targeting PH cannot readily be
291 compared to ours as they used the monocrotaline-induced PH rat model. With this model,
292 there is targeting of the pulmonary circulation rather than RV function by intravenous EPC
293 administration. The effects on the RV were indirect, as pronounced pulmonary effects such as
294 reduced pulmonary arteriole muscularization, reduced pulmonary vessel wall thickening, and
295 an increased number of lung small arterioles were also observed (25) (26). In contrast, in our
296 study, intracoronary EPC administration improved RV function independently of a decrease
297 in the RV afterload.

298 Following intracoronary administration of EPCs, a decrease in the cardiomyocyte area
299 was observed. Gu et al. showed that EPC-derived microvesicles were able to prevent
300 angiotensin II-induced cardiomyocyte hypertrophy *in vitro* (27). The reduced cardiomyocyte

301 area and the tendency to a decreased α/β MHC ratio observed after EPC injection suggests
302 that these cells reversed the RV remodeling. RV reverse remodeling has already been reported
303 in PH patients after lung transplantation (28), pulmonary endarterectomy (29), and balloon
304 pulmonary angioplasty (30). Here, RV hypertrophy seemed to be prevented by a stem cell
305 therapy. Ventricular hypertrophy could be deleterious in case of myocardial ischemia. Indeed,
306 ventricular hypertrophy, combined with increased afterload and increased wall stress, has
307 been shown to lead to increased myocardial oxygen demand and, as a result, myocardial
308 ischemia (31). In this study, the stem cell therapy used may have reversed cardiac remodeling
309 of the RV.

310 EPCs can participate directly in revascularization by repairing damaged vessels or by
311 forming neo-vessels. Their role in the induction of angiogenesis through direct integration
312 into vessels has been demonstrated using murine models of ischemia (10)(11)(12). EPCs
313 administered into myocardial infarcted rats have been shown to secrete paracrine factors that
314 lead to a favorable cardiac remodeling (9)(32). As there is poor cell retention, the effects that
315 we observed were likely due to paracrine secretion by the EPCs. FGF-2, IGF-1, and SDF-1 α
316 are paracrine factors for which levels were increased in ischemic heart after EPC
317 transplantation (9). Furthermore, a positive effect following EPC administration on left
318 ventricle post-myocardial infarction was found to be mediated by IGF-1 (32). Surprisingly,
319 the level of VEGF was upregulated despite a lack of an effect on capillary growth. There may
320 be two explanations for this increase in the level of VEGF: (1) EPCs might give rise to a self-
321 sustaining angiogenic microenvironment at the time of RV injection; (2) the capillary density
322 may not have reached a sufficient level to cover RV needs despite the increase in VEGF
323 expression. Although we have little mechanistic data, we speculate that the observed effect
324 could be a result of one of these paracrine factors.

325 Although RV function determines PH patient survival (1), once the afterload of the
326 RV is alleviated by pulmonary endarterectomy or lung transplantation, the RV has the ability
327 to remodel and return to normal within weeks or months (33)(28). Only targeting the RV
328 would hence provide little benefit, as the pulmonary vasculature would still be obstructed and
329 the RV would therefore still be subject to a high afterload. As the stem cell therapy that we
330 developed here only targets the RV, we aim to use this therapy in combination with current
331 therapies targeting the pulmonary vasculature. The additional targeting of the RV with our
332 EPC-based therapy may prolong the survival of patients.

333

334 **Limitations**

335 One major limitation of our experimental CTEPH model is the lack of a decrease in
336 the capillary density in the RV. We sacrificed the animals at 4 weeks following the
337 establishment of PH, as opposed to Noly et al. (17) who studied the same model after 14
338 weeks, at which time they found a decrease in the capillary density. To overcome the absence
339 of reduced capillary density, a different model could be investigated so as to evaluate the
340 effect of EPCs in the RV without having the pulmonary component. Alternatively, the time of
341 EPC administration could be delayed to obtain a higher level of RV dysfunction, thus leading
342 to the capillary rarefaction, as observed by Noly et al. (17). Finally, heterogeneity of the
343 disease between piglets at T6 makes it difficult to observe significant effects of therapy.
344 However, as the model is stable over the time (17), we are confident that the disease
345 phenotype is not temporary.

346 Although we demonstrated differences between groups considering RVFAC
347 evaluation, we only found significant difference between CTEPH with and without EPC. The
348 lack of power of the study, the low severity of the modeled disease and the early post-

349 injection evaluation may explain these results. However, despite this animal model induced
350 limitations, we found that right ventricular function was significantly improved after EPC
351 injection in CTEPH animals.

352 In this study, peripheral blood collection was only performed in the CTEPH+EPC
353 pigs. As blood collected was less than 7.5% of piglets' blood volume the recovery period
354 lasted less than one week (34). We assume that it did not affect our comparative results.

355 Despite EPCs availability in peripheral blood of PH patients (35) , the main concerns
356 regarding the translation of this cell therapy to clinical studies is the use of autologous cells.
357 First, it could be particularly taxing for severe PH patients to provide a significant blood
358 sample to isolate EPCs. Secondly, the timing between blood sampling, EPC isolation and
359 proliferation, and EPC administration needs to be fully optimized. One solution could be to
360 collect blood following diagnosis of the disease, then to isolate and freeze the EPCs and wait
361 for the patient to be ready for their administration. Thirdly, EPCs isolated from patients with
362 PH may have altered functionality (36) and would require an assessment before use. EPCs
363 isolated from cord blood could be an alternative to autologous EPCs for overcoming all of
364 these limitations. Several studies have shown the superiority of cord blood EPCs over adult
365 EPCs in terms of their proliferative capacity and their ability to create new vessels and to
366 participate in angiogenesis, and their use has already been proposed for several clinical
367 applications (37) (38) (39).

368

369 **Conclusion**

370 Using a porcine model of CTEPH, right intracoronary EPC administration seemed to
371 have a positive effect on RV adaptation to PH. Further studies are needed to determine the
372 best way for administering EPCs, and to confirm these encouraging results in other types of

373 PH models. EPC therapy appears to be a promising therapy to sustain RV function in PH.
374 When used in combination with pulmonary circulation-targeted therapies, this new therapy
375 has the potential to provide clinical benefits for PH patients.

376 **References**

- 377 1. Ghio S, Gavazzi A, Campana C, Inserra C, Klersy C, Sebastiani R, et al. Independent
378 and additive prognostic value of right ventricular systolic function and pulmonary artery
379 pressure in patients with chronic heart failure. *J Am Coll Cardiol.* janv
380 2001;37(1):183-188.
- 381 2. Ryan JJ, Archer SL. Emerging concepts in the molecular basis of pulmonary arterial
382 hypertension: part I: metabolic plasticity and mitochondrial dynamics in the pulmonary
383 circulation and right ventricle in pulmonary arterial hypertension. *Circulation.* 12 mai
384 2015;131(19):1691-1702.
- 385 3. Ryan JJ, Archer SL. The right ventricle in pulmonary arterial hypertension: disorders of
386 metabolism, angiogenesis and adrenergic signaling in right ventricular failure. *Circ Res.*
387 20 juin 2014;115(1):176-188.
- 388 4. Sutendra G, Dromparis P, Paulin R, Zervopoulos S, Haromy A, Nagendran J, et al. A
389 metabolic remodeling in right ventricular hypertrophy is associated with decreased
390 angiogenesis and a transition from a compensated to a decompensated state in
391 pulmonary hypertension. *J Mol Med Berl Ger.* nov 2013;91(11):1315-1327.
- 392 5. Bogaard HJ, Natarajan R, Henderson SC, Long CS, Kraskauskas D, Smithson L, et al.
393 Chronic pulmonary artery pressure elevation is insufficient to explain right heart failure.
394 *Circulation.* 17 nov 2009;120(20):1951-1960.

- 395 6. Ruiter G, Ying Wong Y, de Man FS, Louis Handoko M, Jaspers RT, Postmus PE, et al.
396 Right ventricular oxygen supply parameters are decreased in human and experimental
397 pulmonary hypertension. *J Heart Lung Transplant Off Publ Int Soc Heart Transplant.*
398 févr 2013;32(2):231-40.
- 399 7. Gómez A, Bialostozky D, Zajarias A, Santos E, Palomar A, Martínez ML, et al. Right
400 ventricular ischemia in patients with primary pulmonary hypertension. *J Am Coll*
401 *Cardiol.* oct 2001;38(4):1137-42.
- 402 8. Boyer-Di Ponio J, El-Ayoubi F, Glacial F, Ganeshamoorthy K, Driancourt C, Godet M,
403 et al. Instruction of circulating endothelial progenitors in vitro towards specialized
404 blood-brain barrier and arterial phenotypes. *PloS One.* 2014;9(1):e84179.
- 405 9. Kim S-W, Jin HL, Kang S-M, Kim S, Yoo K-J, Jang Y, et al. Therapeutic effects of late
406 outgrowth endothelial progenitor cells or mesenchymal stem cells derived from human
407 umbilical cord blood on infarct repair. *Int J Cardiol.* 15 janv 2016;203:498-507.
- 408 10. Murohara T, Ikeda H, Duan J, Shintani S, Sasaki K i, Eguchi H, et al. Transplanted cord
409 blood-derived endothelial precursor cells augment postnatal neovascularization. *J Clin*
410 *Invest.* juin 2000;105(11):1527-36.
- 411 11. Flex A, Biscetti F, Iachininoto MG, Nuzzolo ER, Orlando N, Capodimonti S, et al.
412 Human cord blood endothelial progenitors promote post-ischemic angiogenesis in
413 immunocompetent mouse model. *Thromb Res.* mai 2016;141:106-11.
- 414 12. Peng X-G, Bai Y, James JR, Shlapak DP, Ju S. Transplanted Endothelial Progenitor
415 Cells Improve Ischemia Muscle Regeneration in Mice by Diffusion Tensor MR Imaging.
416 *Stem Cells Int.* 2016;2016:3641401.

- 417 13. Simonneau G, Gatzoulis MA, Adatia I, Celermajer D, Denton C, Ghofrani A, et al.
418 Updated clinical classification of pulmonary hypertension. *J Am Coll Cardiol*. 24 déc
419 2013;62(25 Suppl):D34-41.
- 420 14. Mercier O, Tivane A, Dorfmueller P, de Perrot M, Raoux F, Decante B, et al. Piglet
421 model of chronic pulmonary hypertension. *Pulm Circ*. déc 2013;3(4):908-15.
- 422 15. Noly P-E, Guihaire J, Coblenca M, Dorfmueller P, Fadel E, Mercier O. Chronic
423 Thromboembolic Pulmonary Hypertension and Assessment of Right Ventricular
424 Function in the Piglet. *J Vis Exp JoVE*. 4 nov 2015;(105):e53133.
- 425 16. Guihaire J, Haddad F, Boulate D, Capderou A, Decante B, Flécher E, et al. Right
426 ventricular plasticity in a porcine model of chronic pressure overload. *J Heart Lung
427 Transplant Off Publ Int Soc Heart Transplant*. févr 2014;33(2):194-202.
- 428 17. Noly P-E, Haddad F, Ataam JA, Langer N, Dorfmueller P, Loisel F, et al. The importance
429 of Capillary Density/Stroke Work Mismatch for Right Ventricular adaptation to Chronic
430 Pressure Overload. *J Thorac Cardiovasc Surg [Internet]*. 14 juin 2017 [cité 13 juill
431 2017];0(0). Disponible sur: [http://www.jtcvsonline.org/article/S0022-5223\(17\)31183-
432 2/abstract](http://www.jtcvsonline.org/article/S0022-5223(17)31183-2/abstract)
- 433 18. Vonk Noordegraaf A, Haddad F, Bogaard HJ, Hassoun PM. Noninvasive imaging in the
434 assessment of the cardiopulmonary vascular unit. *Circulation*. 10 mars
435 2015;131(10):899-913.
- 436 19. Bensley JG, De Matteo R, Harding R, Black MJ. Three-dimensional direct measurement
437 of cardiomyocyte volume, nuclearity, and ploidy in thick histological sections. *Sci Rep*.
438 6 avr 2016;6:23756.

- 439 20. Vrtovec B, Poglajen G, Lezaic L, Sever M, Socan A, Domanovic D, et al. Comparison
440 of transendocardial and intracoronary CD34+ cell transplantation in patients with
441 nonischemic dilated cardiomyopathy. *Circulation*. 10 sept 2013;128(11 Suppl 1):S42-49.
- 442 21. Chugh AR, Beache GM, Loughran JH, Mewton N, Elmore JB, Kajstura J, et al.
443 Administration of cardiac stem cells in patients with ischemic cardiomyopathy: the
444 SCIPIO trial: surgical aspects and interim analysis of myocardial function and viability
445 by magnetic resonance. *Circulation*. 11 sept 2012;126(11 Suppl 1):S54-64.
- 446 22. Lezaic L, Socan A, Poglajen G, Peitl PK, Sever M, Cukjati M, et al. Intracoronary
447 transplantation of CD34(+) cells is associated with improved myocardial perfusion in
448 patients with nonischemic dilated cardiomyopathy. *J Card Fail*. févr 2015;21(2):145-52.
- 449 23. Li X, Tamama K, Xie X, Guan J. Improving Cell Engraftment in Cardiac Stem Cell
450 Therapy. *Stem Cells Int*. 2016;2016:7168797.
- 451 24. Loisel F, Provost B, Haddad F, Guihaire J, Amsallem M, Vrtovec B, et al. Stem cell
452 therapy targeting the right ventricle in pulmonary arterial hypertension: is it a potential
453 avenue of therapy? *Pulm Circ*. juin 2018;8(2):2045893218755979.
- 454 25. Yip H-K, Chang L-T, Sun C-K, Sheu J-J, Chiang C-H, Youssef AA, et al. Autologous
455 transplantation of bone marrow-derived endothelial progenitor cells attenuates
456 monocrotaline-induced pulmonary arterial hypertension in rats. *Crit Care Med*. mars
457 2008;36(3):873-80.
- 458 26. Xia L, Fu G-S, Yang J-X, Zhang F-R, Wang X-X. Endothelial progenitor cells may
459 inhibit apoptosis of pulmonary microvascular endothelial cells: new insights into cell
460 therapy for pulmonary arterial hypertension. *Cytotherapy*. 2009;11(4):492-502.

- 461 27. Gu S, Zhang W, Chen J, Ma R, Xiao X, Ma X, et al. EPC-derived microvesicles protect
462 cardiomyocytes from Ang II-induced hypertrophy and apoptosis. *PloS One*.
463 2014;9(1):e85396.
- 464 28. Sarashina T, Nakamura K, Akagi S, Oto T, Oe H, Ejiri K, et al. Reverse Right
465 Ventricular Remodeling After Lung Transplantation in Patients With Pulmonary Arterial
466 Hypertension Under Combination Therapy of Targeted Medical Drugs. *Circ J Off J Jpn*
467 *Circ Soc*. 24 févr 2017;81(3):383-90.
- 468 29. Berman M, Gopalan D, Sharples L, Screatton N, Maccan C, Sheares K, et al. Right
469 ventricular reverse remodeling after pulmonary endarterectomy: magnetic resonance
470 imaging and clinical and right heart catheterization assessment. *Pulm Circ*. mars
471 2014;4(1):36-44.
- 472 30. Fukui S, Ogo T, Morita Y, Tsuji A, Tateishi E, Ozaki K, et al. Right ventricular reverse
473 remodelling after balloon pulmonary angioplasty. *Eur Respir J*. mai
474 2014;43(5):1394-402.
- 475 31. Stanton T, Dunn FG. Hypertension, Left Ventricular Hypertrophy, and Myocardial
476 Ischemia. *Med Clin North Am*. janv 2017;101(1):29-41.
- 477 32. Hynes B, Kumar AHS, O'Sullivan J, Klein Buneker C, Leblond A-L, Weiss S, et al.
478 Potent endothelial progenitor cell-conditioned media-related anti-apoptotic,
479 cardiotropic, and pro-angiogenic effects post-myocardial infarction are mediated by
480 insulin-like growth factor-1. *Eur Heart J*. mars 2013;34(10):782-9.
- 481 33. Reesink HJ, Marcus JT, Tulevski II, Jamieson S, Kloek JJ, Vonk Noordegraaf A, et al.
482 Reverse right ventricular remodeling after pulmonary endarterectomy in patients with
483 chronic thromboembolic pulmonary hypertension: utility of magnetic resonance imaging

- 484 to demonstrate restoration of the right ventricle. *J Thorac Cardiovasc Surg.* janv
485 2007;133(1):58-64.
- 486 34. Diehl KH, Hull R, Morton D, Pfister R, Rabemampianina Y, Smith D, et al. A good
487 practice guide to the administration of substances and removal of blood, including routes
488 and volumes. *J Appl Toxicol JAT.* févr 2001;21(1):15-23.
- 489 35. Smadja DM, Mauge L, Sanchez O, Silvestre J-S, Guerin C, Godier A, et al. Distinct
490 patterns of circulating endothelial cells in pulmonary hypertension. *Eur Respir J.* déc
491 2010;36(6):1284-93.
- 492 36. Grisar JC, Haddad F, Gomari FA, Wu JC. Endothelial progenitor cells in cardiovascular
493 disease and chronic inflammation: from biomarker to therapeutic agent. *Biomark Med.*
494 déc 2011;5(6):731-44.
- 495 37. Au P, Daheron LM, Duda DG, Cohen KS, Tyrrell JA, Lanning RM, et al. Differential in
496 vivo potential of endothelial progenitor cells from human umbilical cord blood and adult
497 peripheral blood to form functional long-lasting vessels. *Blood.* 1 févr
498 2008;111(3):1302-5.
- 499 38. Janic B, Arbab AS. Cord blood endothelial progenitor cells as therapeutic and imaging
500 probes. *Imaging Med.* 1 août 2012;4(4):477-90.
- 501 39. Kim J, Jeon Y-J, Kim HE, Shin JM, Chung HM, Chae J-I. Comparative proteomic
502 analysis of endothelial cells progenitor cells derived from cord blood- and peripheral
503 blood for cell therapy. *Biomaterials.* févr 2013;34(6):1669-85.

504

505 **Figure legends**

506 **Figure 1** - (a) Study design. (b) Study design for EPC administration in piglets of the
507 CTEPH+EPC group.

508 **Figure 2** - Proof of concept of EPC intracoronary administration. The location of the EPC-
509 GFP-labeled cells was determined 4 h after their administration in a Sham pig (a, b, c) and 24
510 h after their administration in a CTEPH pig (e,f,g). Anti-GFP staining on HES sections
511 revealed the presence of EPCs in RV myocardium and capillaries (a,b) and in the right upper
512 lobe (c), 4 h after administration EPCs were found in the epicardium of the RV (e,f) and in the
513 right upper lobe (g) 24h after administration.

514

515 **Figure 3** - Figure 3 - Right ventricle and lung function at T10. The assessment of the right
516 ventricular fractional area change revealed an increase in RV contractility in the
517 CTEPH+EPC group compared to the CTEPH group (a). Lung function was assessed by
518 recording mPAP (b) and TPR (c), and it revealed an increase in these parameters in both the
519 CTEPH group and CTEPH+EPC group compared to the Sham group. RV function assessed
520 by pressure-volume loop revealed reduced ventriculo-arterial coupling in the CTEPH group
521 compared to the Sham group (d).The RVSWI did not differ between the groups (e). RVFAC:
522 right ventricular fractional area change; Ees/Ea: right ventricular to pulmonary artery
523 coupling; mPAP: mean pulmonary arterial pressure; TPR: total pulmonary resistance;
524 RVSWI: Right ventricular stroke work indexed. * $p < 0.05$, ** $p < 0.01$.RVFAC: *right*
525 *ventricular fractional area change*; Ees/Ea: *right ventricular to pulmonary artery coupling*;
526 *mPAP: mean pulmonary arterial pressure*; TPR: *total pulmonary resistance*; RVSWI: *Right*
527 *ventricular stroke work indexed*. * $p < 0.05$, ** $p < 0.01$.

528

529 **Figure 4** - Morphometric analysis of the lung and the RV. Measurement of the artery median
530 thickness in the right upper lobe revealed an increase for the CTEPH group and the
531 CTEPH+EPC group compared to the Sham group, while EPC injection did not lead to any
532 change in the median artery thickness (a, b, c, d). The cardiomyocyte study revealed a reduced
533 cardiomyocytes surface area (e), as confirmed by an increase in the α/β myosin heavy chain
534 ratio (f) in the CTEPH+EPC group compared to the CTEPH group. WGA cardiomyocyte
535 surface staining in Sham (g), CTEPH (h), and CTEPH+EPC (i) animals. GFP-labeled EPCs
536 were not detectable in the RV four weeks following their injection, although some were found
537 in the right upper lobe (j) and the spleen (k). * $p<0.05$, ** $p<0.01$, **** $p<0.0001$

538

539 **Figure 5** - Capillary density in the right ventricle at T10. The capillary density quantification
540 was calculated based on immunostaining by CD31 antibody (a,b,c). The capillary density was
541 significantly higher in the CTEPH group and the CTEPH+EPC group compared to the Sham
542 group. Immunostaining by CD31 antibody revealed a tendency for increased capillary density
543 in the CTEPH+EPC group compared to the CTEPH group (d), and this was confirmed by
544 CD31 protein quantification (e). VEGF-A protein quantification revealed its increased
545 expression in both the CTEPH group and the CTEPH+EPC group compared to the Sham
546 group (f). * $p<0.05$, ** $p<0.01$, **** $p<0.0001$

547

548 **Central picture legend**

549 Decreased cardiomyocyte surface area after right intracoronary administration of endothelial
550 progenitor cells in a chronic thromboembolic pulmonary hypertension pig model.

551

552

553 **Video legend**

554 Description of the right intracoronary EPCs administration procedure in a piglet model of
555 CTEPH.

556

557 **Supplemental figure legends**

558 **Supplemental Fig. 1** - EPC characterization. Analysis of EPC expression markers (CD31,
559 CD144 and VEGFR-2) by flow cytometry (a). Uptake of Ac-LDL by EPCs (b). Colony of
560 EPC 8 days after PBMC isolation (c).

561 **Supplemental Fig. 2** - EPC viability post saline resuspension. Positive control represents
562 EPCs resuspended in cell culture media, negative control represents permeabilized EPCs
563 (resuspended with BD Cytofix/Cytoperm™), and NaCl represents EPCs resuspended in NaCl.
564 Ten minutes after their resuspension, a viability staining solution (7AAD) was added to the
565 cells and its fluorescence was analyzed using flow cytometry. FL-3 corresponds to 7AAD
566 fluorescence. 7AAD incorporation between positive control and NaCl condition did not differ
567 showing no cells death after saline resuspension. (n=3)

568 **Supplemental Fig. 3** – Phenotypic characterization of EPCs before and after the
569 establishment of CTEPH: expression of the following markers: CD31 (a), CD144 (b) and
570 VEGFR-2 (c).

571 **Supplemental Fig. 4** – Incorporation of acetylated LDL by EPCs isolated before (a) and after
572 (b) the establishment of CTEPH.

573 **Supplemental Fig. 5** – Wound closure by migration and proliferation of EPCs isolated before
574 and after the establishment of CTEPH.

575 **Supplemental Fig. 6** – Proliferation of EPCs isolated before and after the establishment of
576 CTEPH by measuring dye dilution during their proliferation (CFSE) (a), by analyzing their
577 metabolic activity (MTS assay) (b), and their proliferation by BrdU test (c).

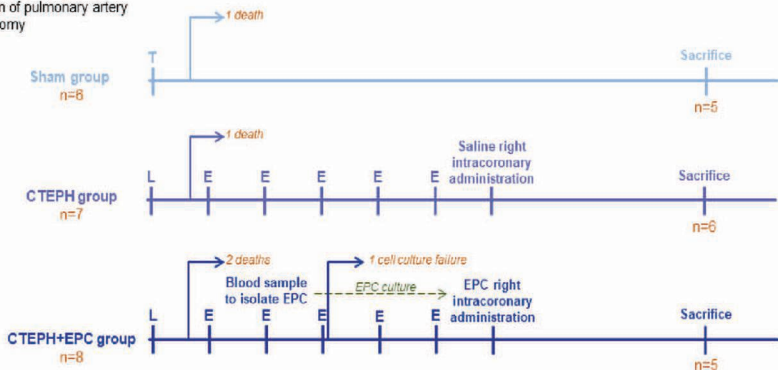
578 **Supplemental Fig. 7** - Cardiac troponin I level before and 1, 4, 24 hours and 4 weeks after
579 right intracoronary EPCs administration ($\mu\text{g/mL}$).

580 **Supplemental Fig. 8** - Right ventricle function. At T10, there was no difference between the
581 CTEPH and CTEPH+EPC groups regarding echographic parameters such as TAPSE (a) and
582 RV free wall strain (b). TAPSE: tricuspid annular plane systolic excursion. ** $p < 0.01$

583 **Supplemental Fig. 9** - Analysis of GFP expression in RV by Western Blot 4 weeks after right
584 intracoronary administration of the EPCs.

a)
 L: left pulmonary artery ligation
 E: embolization of pulmonary artery
 T: left thoracotomy

Study design



Time line

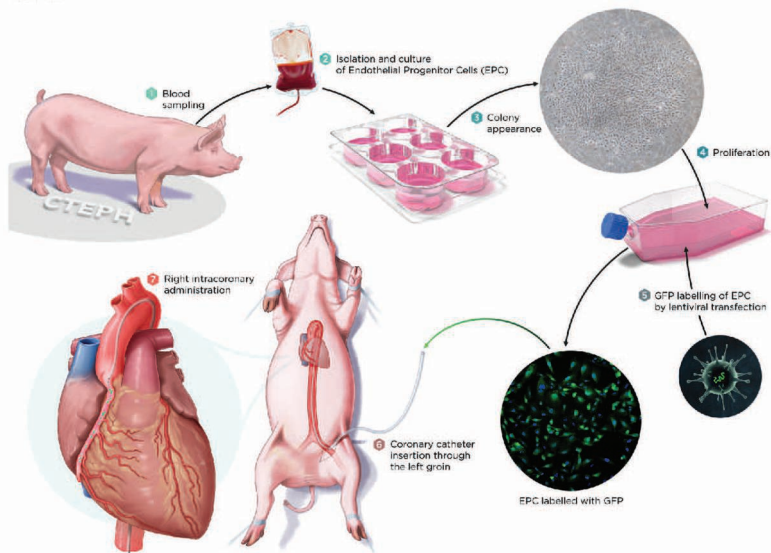


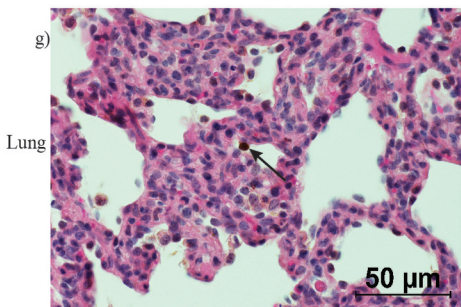
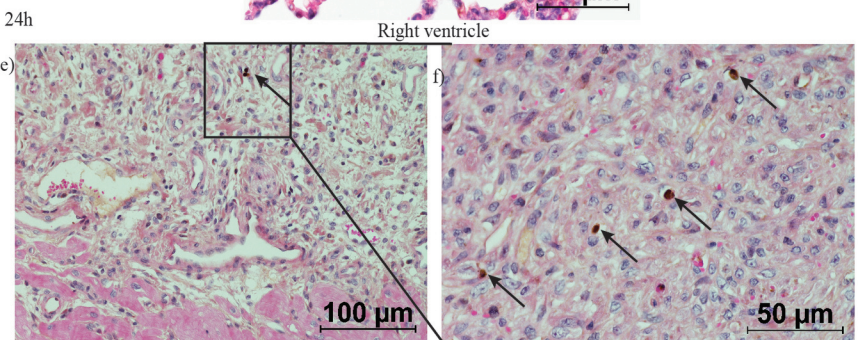
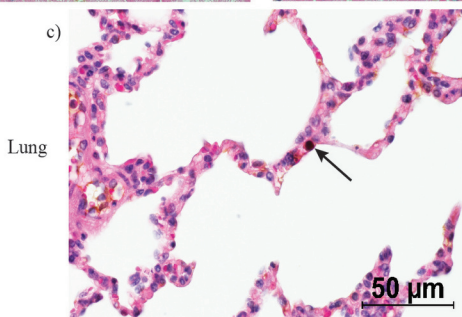
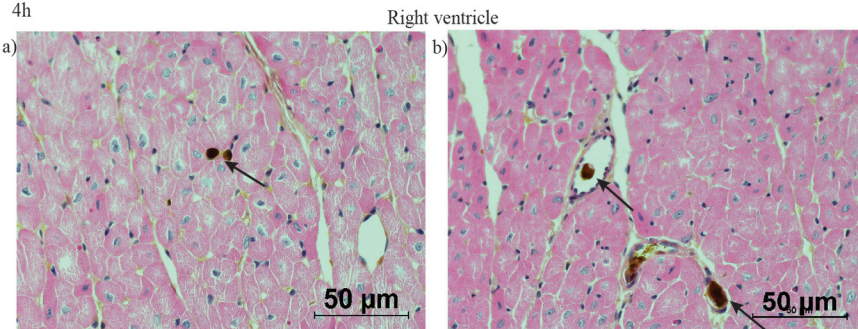
Assessment

Right heart catheterization
 Echocardiography
 Pressure - Volume loops
 Pathology
 (capillary density, cardiomyocyte surface area, pulmonary artery media thickness, protein and ARN expression)

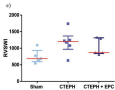
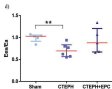
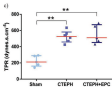
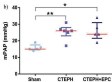
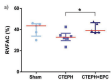


b)

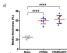




- Sham
- CTEPH
- CTEPH+EPC



- Sham
- CTRH
- ▲ CTRH+IPC



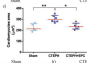
Sham



CTRH



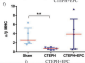
CTRH+IPC



Sham

CTRH

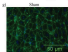
CTRH+IPC



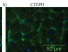
Sham

CTRH

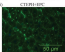
CTRH+IPC



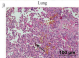
Lung



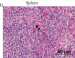
Lung



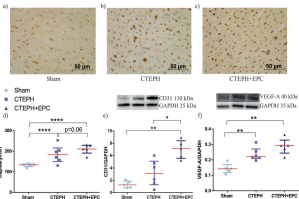
Lung



100 µm



50 µm



	Sham group (n=5)	CTEPH group (n=6)	CTEPH+EPC group (n=5)
Body weight (kg)	39.3 (37.8-43.65)	34.4 (32.25-34.85)	28 (26.20-34.60)
Body surface area	1.11 (1.08-1.20)	1 (0.97-1.01)	0.89 (0.85-1.01)
Right heart catheterization			
mPAP (mmHg)	15 (14.5-17.5)	26 (23-28)	24 (21.5-31)
TPR (dyn.s.cm ⁻⁵)	211.6 (161.1-289.5)	525.8 (458.1-581.4)	510.9 (451.7-672.1)
Cardiac output indexed	5.53 (4.97-5.75)	3.98 (3.65-4.43)	4.12 (3.83-4.94)
Echocardiography			
RVFAC (%)	43.5 (33.75-45.48)	32.7 (29.5-36.5)	39 (37.25-46.5)
TAPSE (mm)	21 (19.5-21)	15.5 (13.75-17.25)	16 (15.5-17)
RV free wall strain (%)	33 (28.6-36)	19.5 (15.5-27.25)	24 (23.5-29)
Conductance measurements			
Ees/Ea	1.03 (0.92-1.05)	0.69 (0.56-0.83)	0.88 (0.67-1.20)

Table 1 - Hemodynamic and echocardiographic measurements of the Sham, CTEPH and CTEPH+EPC at 10 weeks (median (IQR)).